Geophys. J. Int. (2007) **170,** 460–467 doi: 10.1111/j.1365-246X.2007.03399.x

Non-linear crustal corrections in high-resolution regional waveform seismic tomography

Federica Marone* and Barbara Romanowicz

Berkeley Seismological Laboratory, University of California, 215 *McCone Hall* #4760, *Berkeley* CA 94720-4760, *USA. E-mail: federica@seismo.berkeley.edu*

Accepted 2007 February 9. Received 2007 February 9; in original form 2006 February 13

SUMMARY

We compare 3-D upper mantle anisotropic structures beneath the North American continent obtained using standard and improved crustal corrections in the framework of Non-linear Asymptotic Coupling Theory (NACT) applied to long period three component fundamental and higher mode surface waveform data. Our improved approach to correct for crustal structure in high-resolution regional waveform tomographic models goes beyond the linear perturbation approximation, and is therefore more accurate in accounting for large variations in Moho topography within short distances as observed, for instance, at ocean–continent margins. This improved methodology decomposes the shallow-layer correction into a linear and non-linear part and makes use of 1-D sensitivity kernels defined according to local tectonic structure, both for the forward computation and for the computation of sensitivity kernels for inversion. The comparison of the 3-D upper mantle anisotropic structures derived using the standard and improved crustal correction approaches shows that the model norm is not strongly affected. However, significant variations are observed in the retrieved 3-D perturbations. The largest differences in the velocity models are present below 250 km depth and not in the uppermost mantle, as would be expected. We suggest that inaccurate crustal corrections preferentially map into the least constrained part of the model and therefore accurate corrections for shallow-layer structure are essential to improve our knowledge of parts of the upper mantle where our data have the smallest sensitivity.

Key words: crustal structure, lateral heterogeneity, surface waves, tomography.

1 INTRODUCTION

Body and surface wave data sets used in mantle seismic tomography are sensitive to crustal structure (Fig. 1), but due to finite depth resolution cannot resolve details within the crust. Accurate crustal corrections are therefore essential to prevent mapping crustal features into mantle tomographic images and thus biasing the modelled structure. In seismic tomographic studies, the effect of shallow-layer features is often removed from the data by assuming an *a priori* crustal model and applying linear perturbation corrections (Fig. 2a) (e.g. Ekström & Dziewonski 1998; Ritsema *et al.* 1999). Lateral variations in Moho depth can, however, be fairly large even over short distances, as for instance at ocean–continent margins, and consequently the assumption of linearity is questionable. In fact, Montagner & Jobert (1988) showed that the non-linearity of shallow-layer corrections is often not negligible even at long periods. Going beyond the linear perturbation approximation and accounting for the crustal structure in a more accurate way is therefore, together with current theoretical advances and massive data sets, an indispensable ingredient towards a new generation of high resolution-tomographic earth models.

Apart from Montagner's work, the Partitioned Waveform Inversion approach (Nolet 1990; Van der Lee & Nolet 1997) represents one of the first attempts to account for the lateral sensitivity variation of surface waves introduced by strongly heterogeneous Earth (in particular crustal) structure. One of the advantages of this algorithm is that it allows the use of different sensitivity kernels appropriate for the 1-D average Earth structure along each single path. This procedure brings a significant advance for paths traversing a relatively homogeneous region. Because it involves averaging of the structure along the source–receiver path, it, however, remains inadequate for paths crossing diverse tectonic provinces.

Boschi & Ekström (2002) defined a set of 1-D sensitivity kernels on a $5^\circ \times 5^\circ$ grid for a 3-D model that includes a realistic map of the crust, and used them in the framework of the Jeffreys-Wentzel-Kramers-Brillouin approximation to constrain the global upper mantle transverse isotropic structure from fundamental mode phase velocity measurements. This approach accounts for lateral variations in surface-wave sensitivity associated with the crust, and

*Now at: Paul Scherrer Institut, Swiss Light Source/WLGA 135, 5232 Villigen, Switzerland. E-mail: federica.marone@psi.ch.

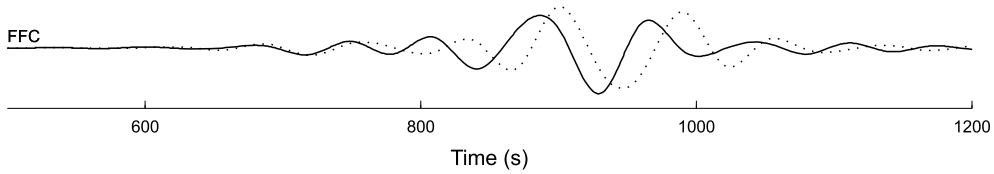

Figure 1. Band-pass filtered (corner frequencies of 80 and 250 s) transverse component synthetic seismograms computed with different crustal structures: PREM (solid) and CRUST2.0 (dotted). The same 3-D radial anisotropic upper mantle model has been used for the two synthetics. The computation has been done for an event in Mexico (January 11, 1997 - $M_w = 7.1$) and the Global Seismograph Network station (Flin Flon, Canada).

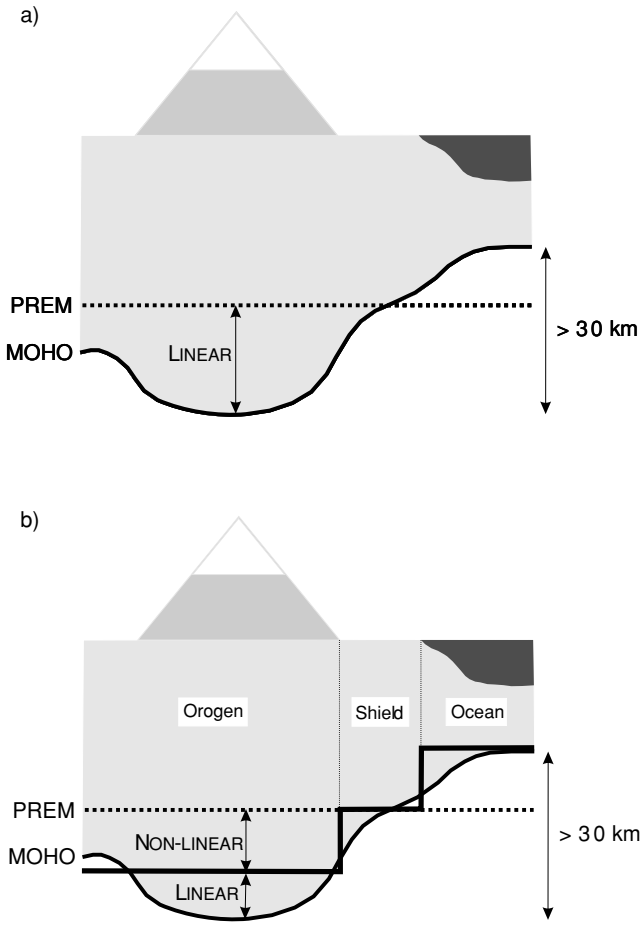

Figure 2. Crustal corrections-(a) Traditional approach, (b) Approach originally proposed by Montagner & Jobert (1988), where the shallow-layer correction is decomposed into a linear and a non-linear part.

especially with the large variations of its thickness over short horizontal distances. Their results show that the lateral dependence of the surface-wave sensitivity kernels has a significant effect on the absolute amplitude of the anomalies, which should not be neglected if the aim is higher resolution upper mantle images. This procedure is, however, computationally too intense, to be used if the complete long-period seismogram (including both fundamental mode and overtone waveforms) is accurately modelled taking into account mode coupling across different dispersion branches, as in the non-linear asymptotic coupling approach (NACT, Li & Romanowicz 1995).

Recently, Zhou *et al.* (2005) derived 2-D boundary sensitivity kernels for lateral variations in crustal thickness based upon first order Born approximation and showed that finite frequency crustal effects are not negligible in long-period surface wave dispersion studies, especially for paths along continental–ocean margins. However, as noticed in the past (Montagner & Jobert 1988), they also confirmed that linear perturbation theory is not sufficiently accurate to make reliable crustal corrections in regions with large topography on the Moho discontinuity. The finite frequency boundary sensitivity kernels they derived do not reliably account for finite frequency effects if large variations on the Moho depth are present and therefore they eventually followed a similar approach as Boschi & Ekström (2002). Incorporation of finite frequency effects beyond the first order Born approximation would require higher order perturbation theory (Lognonné & Romanowicz 1990; Lognonné 1991) or a more comprehensive numerical treatment (e.g. Komatitsch & Tromp 1999).

In this study, we propose a simplification of Boschi & Ekström (2002) crustal correction technique, suitable to be used in seismic waveform tomography within a reasonable computational timeframe. We implemented the approach discussed in Appendix A of Montagner & Jobert (1988), where the shallow-layer correction is decomposed into a linear and a non-linear part (Fig. 2b). Here, we outline the method and present its application to a regional tomographic study of the North American continent. In particular, we assess and discuss the impact of this methodological improvement on the retrieved model.

2 METHOD

We apply a full waveform tomographic method based on NACT (Li & Romanowicz 1995), which permits the inversion of entire long-period seismograms in the time domain (including fundamental mode, overtones and body wave portions of the record) simultaneously for perturbations in the isotropic *S*-velocity structure and the anisotropic parameter $\xi = \frac{v_{SH}^2}{v_{SV}^2}$, in one step, without the intermediate stage of calculating phase velocity maps as a function of frequency. NACT is a normal-mode perturbation approach that takes into account coupling between modes both along and across dispersion branches. The asymptotic calculation of this coupling allows the computation of 2-D broad-band sensitivity kernels that reproduce the sensitivity of body waveforms to structure along and around the ray geometrical path in the vertical plane containing the source and the receiver, more accurately than the classical path-average approximation (Woodhouse & Dziewonski 1984). This body wave character reflected in the 2-D kernels is also important to accurately model the waveforms of surface wave overtones. In contrast, traditional methods, such as the Partitioned Waveform Inversion technique, based on path average approximation and infinite frequency 'ray theory', rely on 1-D sensitivity kernels, an assumption which is strictly valid only for fundamental mode surface waves, in the absence of focusing effects in the horizontal plane, which we also do not consider here. The details of the application of our approach to the North American region and the resulting 3-D upper mantle regional anisotropic model are presented in a separate paper (Marone

et al. 2006). Here, we focus the discussion on a particular aspect: the correction for crustal structure.

We follow the approach originally proposed by Montagner & Jobert (1988) for fundamental mode Rayleigh and Love wave-phase velocity measurements, where the shallow-layer correction is decomposed into a linear and a non-linear part. As in traditional approaches, we assume an *a priori* 3-D crustal model, CRUST2.0 (Bassin *et al.* 2000). Since the data sensitivity to the topography of discontinuities is significantly larger than to the 3-D heterogeneous elastic crustal structure, we only consider and correct for variations in Earth's topography and Moho depth in the chosen *a priori* model with respect to the 1-D global reference model (GRM). In contrast to traditional procedures, for the shallow-layer correction we do not use, throughout the study region, the same 1-D sensitivity kernel computed for the 1-D GRM (Fig. 2a). We define instead a set of different 1-D local reference models (LRM) which we assign to each point (θ, ϕ), along the source-station path, according to the local crustal structure (e.g. ocean, shield, orogen) in the selected *a priori* 3-D crustal model (Fig. 2b). At each point, the correction is then split into a non-linear term, for the depth difference, if any, between the 1-D LRM and the global 1-D reference model (GRM), and a linear term, for the difference between the discontinuities in the chosen *a priori* 3-D crustal model and in the selected 1-D LRM (Fig. 2b).

The local frequency perturbation for the multiplet pair kk' due to variations in the 3-D heterogeneous structure with respect to the 1-D GRM is defined as:

$$\delta\omega^{\mathrm{GRM}}_{kk'}(\theta,\phi) = \omega_{kk'}(\theta,\phi) - \omega^{\mathrm{LRM}}_{kk'}(\theta,\phi) + \omega^{\mathrm{LRM}}_{kk'}(\theta,\phi) - \omega^{\mathrm{GRM}}_{kk'} = \cong \underbrace{\delta\omega^{\mathrm{LRM}}_{kk'}(\theta,\phi)}_{\text{linear}} + \underbrace{\omega^{\mathrm{LRM}}_{kk'}(\theta,\phi) - \omega^{\mathrm{GRM}}_{kk'}}_{\text{non-linear}} \quad (1)$$

where $\omega_{kk'}(\theta, \phi)$ is the local eigenfrequency of the 3-D heterogeneous model comprising the chosen *a priori* 3-D crustal model, and:

$$\delta\left(\omega^{\mathrm{LRM}}_{kk'}(\theta,\phi)^2\right) = \int_0^a \delta m^{\mathrm{LRM}}(\theta,\phi,r) M^{\mathrm{LRM}}_{kk'}(\theta,\phi,r) r^2 dr - \sum_d r^{\mathrm{LRM}^2}_d(\theta,\phi) h^{\mathrm{LRM}}_d(\theta,\phi) H^{\mathrm{LRM}^d}_{kk'}(\theta,\phi) \quad (2)$$

with $\delta m^{\mathrm{LRM}}(\theta, \phi, r)$ and $h^{\mathrm{LRM}}_d(\theta, \phi)$ representing the deviation of the elastic parameters and undulation of the dth discontinuity with respect to their values in the 1-D LRM. $M^{\mathrm{LRM}}_{kk'}(\theta, \phi, r)$ and $H^{\mathrm{LRM}d}_{kk'}(\theta, \phi)$ are the respective local sensitivity kernels for the multiplet pair kk', which together with the eigenfrequencies $\omega^{\mathrm{LRM}}_{kk'}$ have been previously computed and stored. $r^{\mathrm{LRM}}_d(\theta, \phi)$ is the unperturbed radius of the dth discontinuity in the 1-D LRM. $\delta\omega^{\mathrm{GRM}}_{kk'}(\theta, \phi)$ as computed in eq. (1), instead of eq. (14) of Li & Romanowicz (1995), is then used in the forward problem to calculate synthetic seismograms and corresponding partial derivatives in the NACT framework (eqs (10)–(13) and eqs (21)–(22)—Li & Romanowicz (1995)). These partial derivatives and the residuals between computed synthetics and observed seismograms will then build the inverse problem, which will be solved for the 3-D radial anisotropic structure (Panning & Romanowicz 2006).

3 LOCAL 1-D SENSITIVITY KERNELS

In this study, we have subdivided our target region into five tectonic provinces (Fig. 3) and constructed five corresponding 1-D LRMs (Fig. 4), simplifying the crustal structure proposed in CRUST2.0 (Bassin *et al.* 2000) and using Preliminary Reference Earth Model

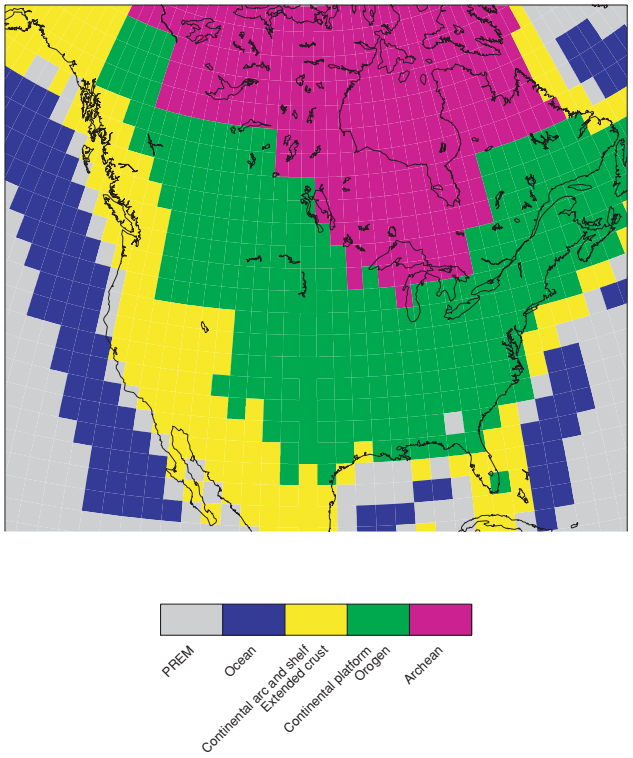

Figure 3. Subdivision of North America into five crustal/tectonic provinces following CRUST2.0.

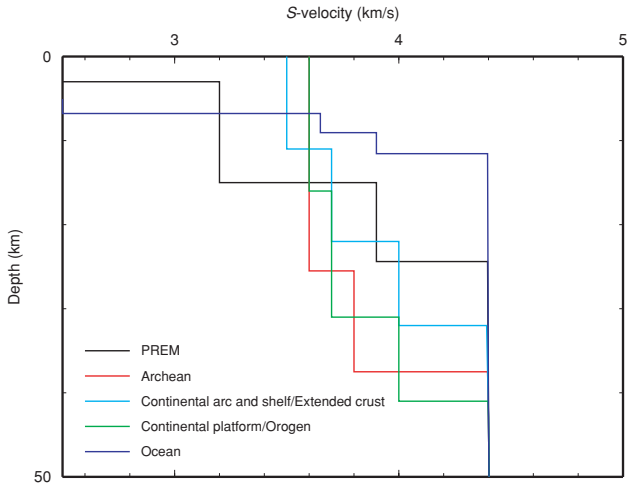

Figure 4. 1-D local reference models (LRM) for crustal corrections in different tectonic environments.

(PREM) (our 1-D GRM) for the velocities beneath the Moho. In particular, we characterized North America by a northeastern Archean core (Moho at 37.5 km depth and relatively reduced lower crustal velocities) surrounded by a region dominated by a continental platform and orogens (41 km thick crust and average crustal velocities). We describe most coastal areas and regions characterized by an extended crust by a transitional model (32 km thick crust and average crustal velocities) and the offshore regions by a standard oceanic structure. Our 1-D GRM, PREM (Dziewonski & Anderson 1981), is assigned to the remaining areas (mostly at the ocean/continent margin).

We compute the depth $M_{kk'}(r)$ and discontinuity $H^d_{kk'}$ sensitivity kernels for each 1-D LRM thus defined. Large differences

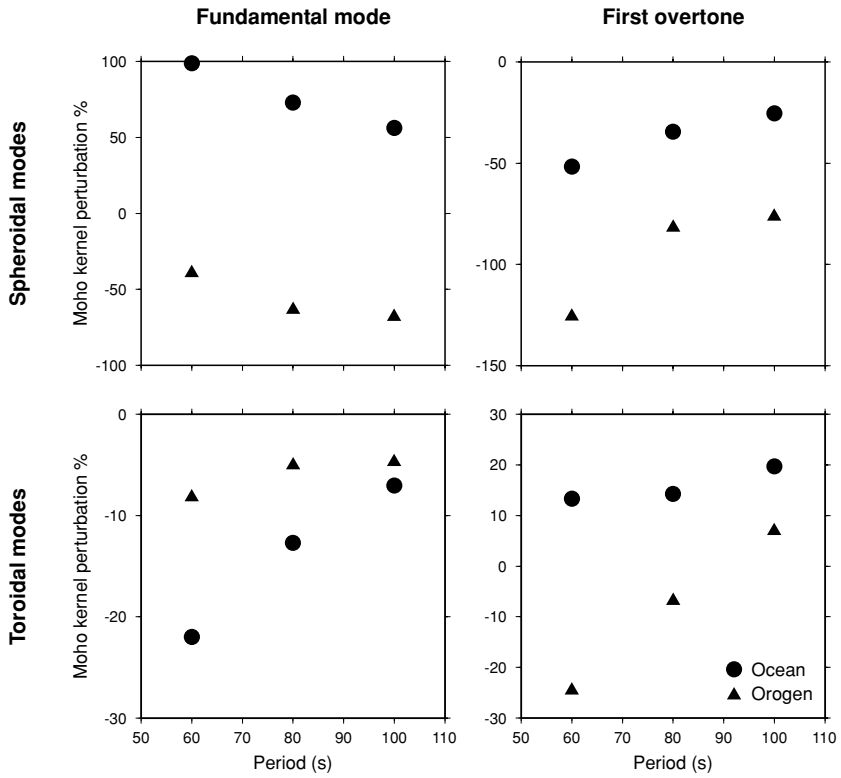

Figure 5. Perturbation of spheroidal (top) and toroidal (bottom) mode sensitivity kernels for Moho depth $H_{kk'}$ for 2 different 1-D models shown in Fig. 4 (ocean (circle), orogen (triangle)) with respect to PREM at three different periods, on the left for the fundamental mode, on the right for the first overtone.

in the sensitivity kernels for Moho depth are observed both for fundamental and higher modes (Fig. 5). As expected, variations are larger at short periods (larger than 100 per cent for the first spheroidal overtone), but even for a period of 100 s, differences reach 50 per cent both for fundamental and higher spheroidal modes. Different crustal structures, as present in the 1-D LRMs used, have a large effect also on the depth-sensitivity kernels $M_{\mathrm{kk'}}(r)$ (Figs 6a and b, 7a and b), especially at short period ($T = 60$ s) both for fundamental and higher toroidal modes. The observed variations arise uniquely from the differences in the shallow structure, since the velocities beneath the Moho are the same in all 1-D LRMs. As expected, the largest effect of the crustal structure on the depth sensitivity kernels is observed immediately beneath the Moho discontinuity. Significant differences in $M_{kk'}(r)$ are, however, also present well down into the upper mantle (200–400 km depth), in particular for toroidal modes. Similar conclusions can also be drawn from the comparison (Figs 6c and d and 7c and d) of the depth sensitivity kernels for PREM and a modified version of PREM, where the Moho discontinuity has been moved to 35 km depth, while the other interfaces and the crustal and mantle velocities are not changed. Accordingly, although using the 1-D LRMs to correct for the shallow-structure will mainly affect the uppermost mantle, we also expect the deeper structure to be influenced. This comparison of depth sensitivity kernels for 1-D models with different crustal structures suggests that inaccurate correction for shallow-layer features can map significantly deeper than just in the top upper mantle.

Our 3-D *a priori* crustal model for shallow-layer corrections consists of two discontinuities: the Earth's topography and Moho interface. The Earth's topography is modelled according to ETOPO-5 (National Geophysical Data Center 1988), the Moho interface according to CRUST2.0 (Bassin *et al.* 2000). The accuracy of the shallow-layer correction, in addition to the approach used to compute it, obviously also depends on the accuracy of the chosen crustal model. The locations at which crustal thickness has been determined with an accuracy of a few kilometers or less in refraction and reflection experiments or in receiver function studies are unevenly distributed, with the highest density for continents in the Northern Hemisphere. CRUST2.0 is currently the available global crustal model based on the most up-to-date compilation of such data, with the densest sampling in North America and Eurasia. For the maximum resolution of this study (in the order of 500 km), the accuracy of CRUST2.0 should be sufficient. However, one of the requirements for future higher-resolution models will definitely be improved knowledge of shorter wavelength crustal structures.

4 MODEL ASSESSMENT

The aim of this paper is not the discussion of the obtained 3-D anisotropic structure in terms of tectonic processes, which is the topic of a separate publication (Marone *et al.* 2006). Here, we focus, instead, on a qualitative and quantitative comparison of the models obtained using different approaches for the shallow-layer corrections.

The 1-D LRMs are used in the forward problem, both for the synthetics and partial derivative matrix computation. To evaluate the significance of these more correct sensitivity kernels in the various parts of the problem, we computed the synthetics and partial derivative in four different ways (Table 1), ran a similar inversion in all cases and compared the derived 3-D anisotropic structure. The two extreme models have been derived using either 1-D PREM sensitivity kernels (Model 4) or the sensitivity kernels for the 1-D

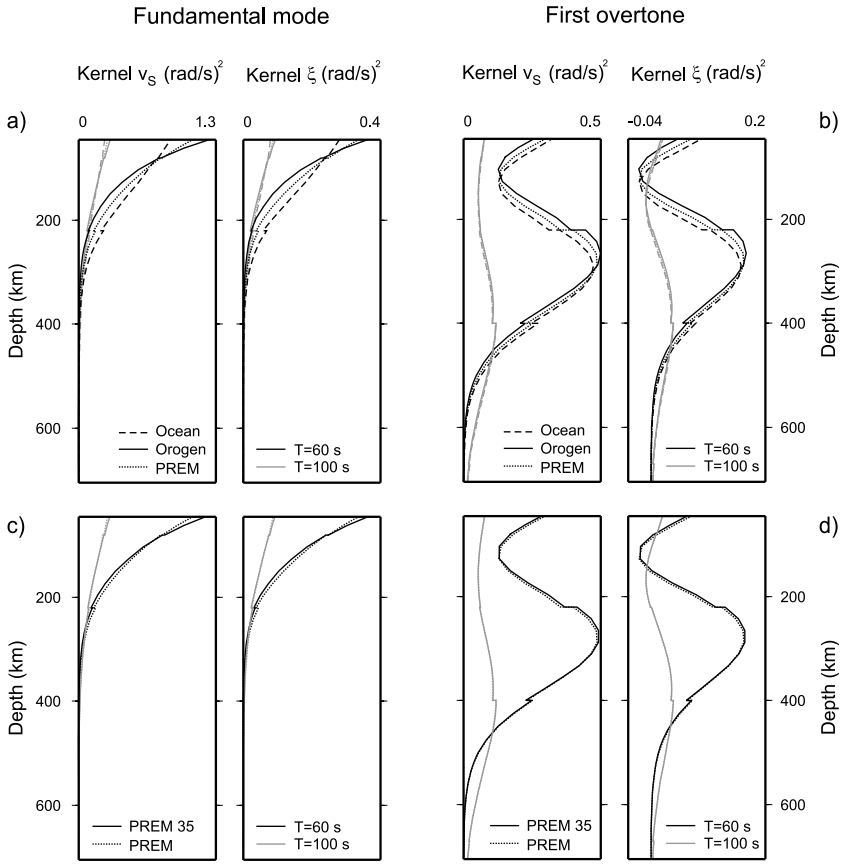

Figure 6. Comparison of toroidal mode depth-sensitivity kernels $M_{kk'}(r)$, on the left for isotropic v_S, on the right for ξ - (a) For the fundamental mode and for three different 1-D models shown in Fig. 4 (PREM (dotted), ocean (dashed), orogen (solid)) at two different periods (black: $T = 60$ s, grey: $T = 100$ s), (b) The same as in (a), but for the first overtone, (c) For the fundamental mode and for PREM (dotted) and a modified version of PREM (solid), where the Moho discontinuity has been moved to 35 km, (d) The same as in (c), but for the first overtone.

LRMs (Model 1) for both the synthetics and partial derivative matrix computation. For Model 2, we used the sensitivity kernels for the 1-D LRMs only for the synthetics computation, while keeping 1-D PREM kernels for the partial derivative matrix calculation. The last model (Model 3) has been derived using the improved sensitivity kernels only to account for the discontinuities perturbations, in the synthetics computation, while for the elastic mantle structure and the partial derivatives, 1-D PREM sensitivity kernels have been adopted.

In terms of model norm, the rms amplitude of the isotropic parts of Model 2, Model 3 and Model 4 (Fig. 8a) are similar throughout the upper mantle, with a positive peak around 100 km depth. The rms amplitude of Model 1 has a more constant character down to 180 km, with a larger rms value above 50 km and a smaller one below. The rms amplitude of the anisotropic part of the models is also characterized by strong similarities, although the variations among the models are larger than for the isotropic structure.

While the 1-D average model structure is robust and does not strongly depend on the crustal correction approach used, the 3-D perturbations in the four derived anisotropic models differ significantly. Fig. 8(b) displays, as a function of depth, the correlation coefficient between Model 1 and the other three models for both the isotropic and anisotropic 3-D structure. The largest differences are observed between Model 1 and Model 2, for which different sensitivity kernels have been used for partial derivative computations. For the isotropic velocity structure, an excellent correlation is observed for the uppermost mantle, but it degrades beneath 300 km depth. For the anisotropic structure, the correlation coefficient is, on average, larger than for the isotropic velocity structure for the entire upper mantle and the largest differences are observed in the top 200 km. These observations indicate that the use of appropriate sensitivity kernels is important in all parts of the problem: it influences not only the calculation of synthetics, but has an even more important effect on partial derivative computations (Fig. 8b).

In addition, Fig. 8(b) illustrates a surprising result. For the isotropic *S*-velocity structure, the largest differences in the models obtained using different approaches for the crustal corrections are observed at depths larger than 300 km and not in the uppermost mantle as intuitively expected from comparison of different 1-D sensitivity kernels (Figs 5, 6a, b, 7a and b). First, these observations indicate that different 1-D sensitivity kernels for the shallow-layer corrections do not only influence the retrieved structure immediately below the Moho, but that they affect the obtained 3-D model down to the transition zone. The more consistent formulation of the inverse problem arising from the more accurate modelling of the shallow-layer structure causes rearrangements throughout the model space. Second, the top 300 km of the isotropic part of the model corresponds to the best constrained portion of the inverse problem, thanks to the largest sensitivity of the fundamental modes for the isotropic velocity structure at these depths. We suggest that inaccurate crustal corrections preferentially map into the least constrained part of the model, in our case biasing the deep upper mantle isotropic structure

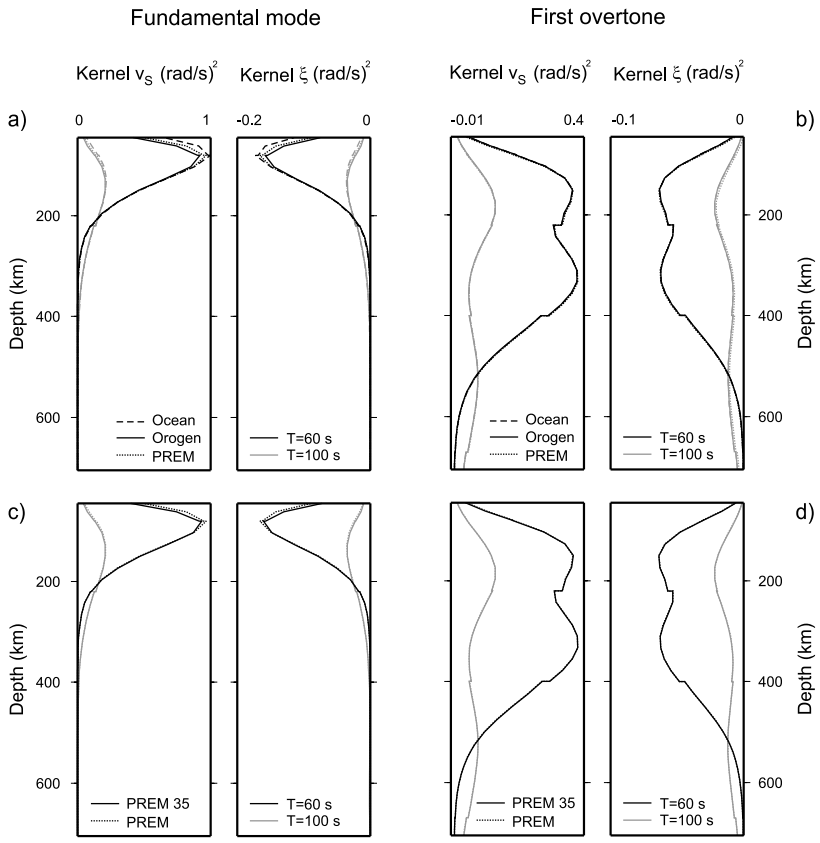

Figure 7. Comparison of spheroidal mode depth sensitivity kernels $M_{kk'}(r)$, on the left for isotropic v_S, on the right for ξ - (a) For the fundamental mode and for three different 1-D models shown in Fig. 4 (PREM (dotted), ocean (dashed), orogen (solid)) at two different periods (black: $T = 60$ s, grey: $T = 100$ s), (b) The same as in (a), but for the first overtone, (c) For the fundamental mode and for PREM (dotted) and a modified version of PREM (solid), where the Moho discontinuity has been moved to 35 km, (d) The same as in (c), but for the first overtone.

Table 1. Type of 1-D sensitivity kernels used for synthetics and partial derivative matrices computation for different test models. Using 1-D sensitivity kernels for the global reference model (GRM), PREM in our case, implies utilizing the same eigenfunctions throughout the study region. In contrast, using sensitivity kernels for local reference models (LRM) involves the use of different eigenfunctions in different regions computed according to the local crustal structure.

Sensitivity kernels for:	Synthetics		Partial derivatives
	Discontinuities	Elastic mantle structure	
Model 1	LRMs	LRMs	LRMs
Model 2	LRMs	LRMs	GRM
Model 3	LRMs	GRM	GRM
Model 4	GRM	GRM	GRM

and many of the anisotropic features. These results therefore imply that accurate corrections for shallow-layer features are important to improve our knowledge of parts of the upper mantle not optimally constrained by the available data.

Fig. 9 visually compares the 3-D perturbations of the isotropic structure in Model 1 and Model 4 at depths where the largest discrepancies are observed (around 300 km, Fig. 8b). Both models show positive anomalies beneath the northeastern part of the continent at 250 km depth as well as deeper fast mantle material in the western United States. Despite similarities, these two models differ in several details. Most remarkably Model 1 shows a much more pronounced high velocity anomaly at 300–350 km depth beneath the Western US than Model 4. This feature correlates well with the expected position of the subducted part of the Juan de Fuca plate in the North as suggested by higher resolution regional body wave tomographic studies (e.g. Humphreys & Dueker 1994; Bostock & VanDecar 1995) and could indicate the presence of remanents of the Farallon plate in the South. In addition, the base of the North American craton is sharper in Model 1, where positive velocity anomalies give way to a low-velocity region, possibly the asthenosphere, beneath 250–300 km depth, a feature not present in Model 4. Finally although it is also visible in Model 1, the slab window in the Western US (Dickinson & Snyder 1979) is more pronounced in Model 4.

Despite the observed differences, models derived using the traditional approach and more sophisticated crustal corrections fit the used waveform data almost as well (Fig. 10, 67.0 per cent and 66.0 per cent variance reduction, respectively). In both cases, the largest improvement in data fit is observed after the first iteration, while for additional iterations, the curve quickly flattens. Although using 1-D sensitivity kernels tuned according to the tectonic structure

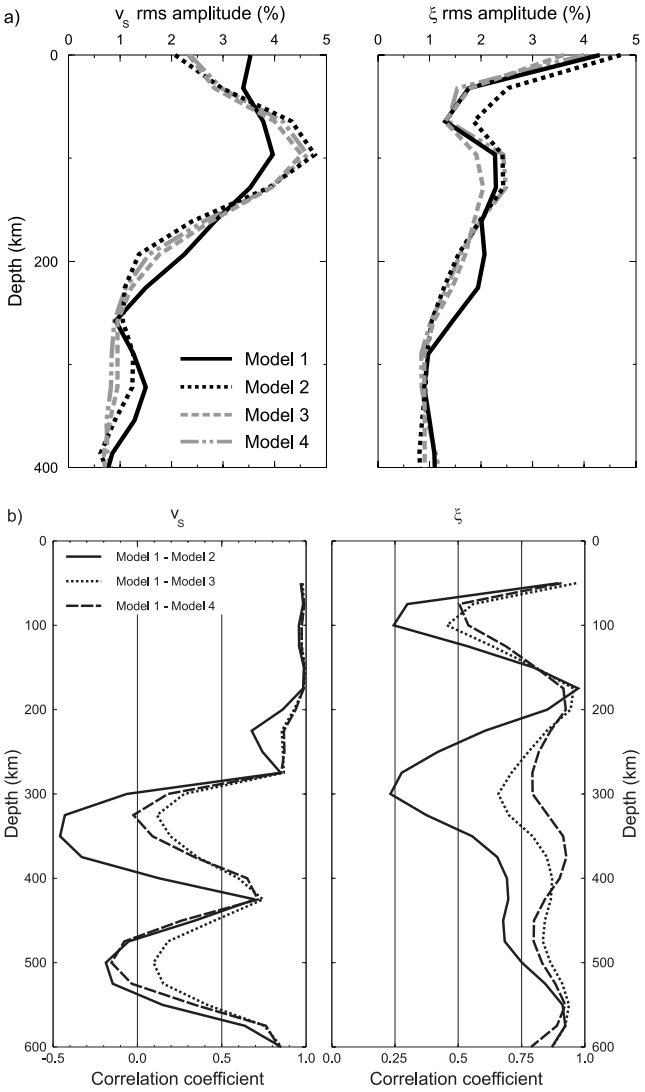

Figure 8. Rms amplitude (a) and correlation coefficient (b) for the isotropic *S*-velocity (on the left) and anisotropic (on the right) structure for four different models (see text for details).

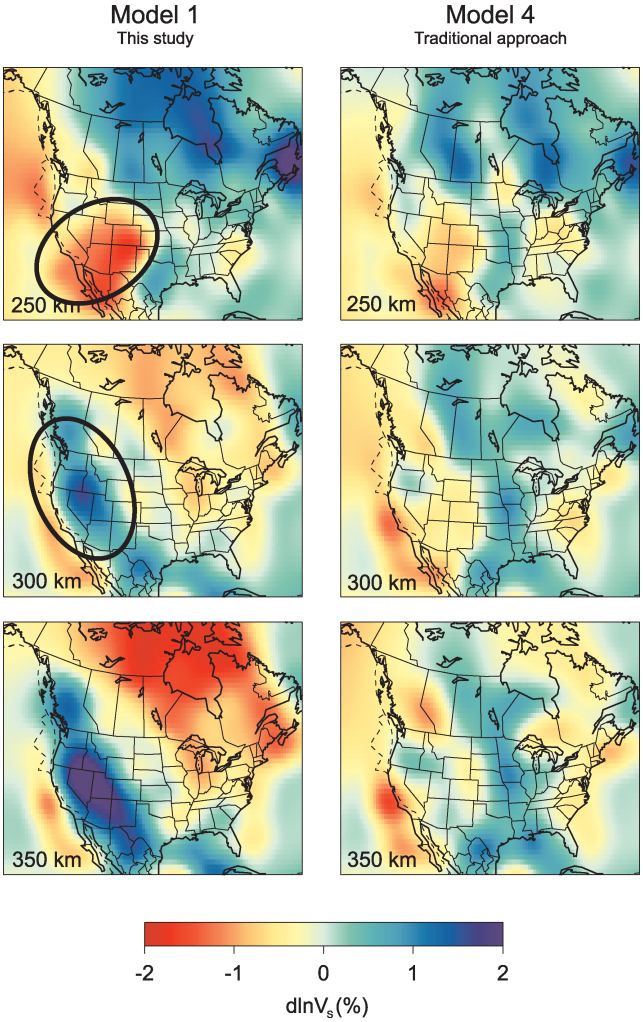

Figure 9. 3-D perturbations in the isotropic *S*-velocity structure at three different depths of two models (Model 1 and Model 4) obtained with different approaches for the crustal correction (Table 1): the traditional procedure with 1-D PREM sensitivity kernels on the right and the improved procedure of this study which makes use of 1-D local sensitivity kernels on the left. These anomalies are with respect to average. The ellipses indicate features discussed in the text.

does not result in models fitting the data significantly better, such an approach, which is theoretically more accurate in accounting for large discontinuity topography, represents a way to introduce *a priori* constraints into the problem, reducing the non-uniqueness of the inversion and discriminating between different models which fit the data equally well. Improved crustal correction techniques, such as the procedure presented in this paper, should therefore be preferred and routinely applied in high-resolution 3D seismic tomography.

5 CONCLUSIONS

We have presented a new approach to correct for unmodelled crustal features in high-resolution regional waveform tomographic models, which goes beyond the linear perturbation approximation and is therefore more accurate in accounting for large variations in Moho topography within short distances as observed at ocean–continent margins. This new implementation is based on the approach originally proposed by Montagner & Jobert (1988) for fundamental mode phase velocity measurements: it decomposes the shallow-layer correction into a linear and a non-linear term and makes use of 1-D sensitivity kernels defined according to the local tectonic structure.

The comparison of 1-D sensitivity kernels computed for 1-D earth models characterized by different crustal features but equal structures below the Moho shows large variations in the kernel for Moho perturbations even at long periods (larger than 50 per cent for both fundamental and higher modes). In addition, significant differences are also observed in depth sensitivity kernels as deep as 250–300 km. We show that the use of different sensitivity kernels is important in all parts of the tomographic problem, with a particularly dominant effect on partial derivative computations.

On the one hand, the comparison of the 3-D anisotropic structures derived using 1-D sensitivity kernels for PREM and LRMs shows that the model norm is well constrained and rather small differences are observed. On the other hand, larger variations are observed in the retrieved 3-D perturbations. The strongest differences in the velocity model are present below 250 km depth and not in the top upper mantle as would be expected. We suggest that inaccurate crustal corrections preferentially map into the least constrained part of the

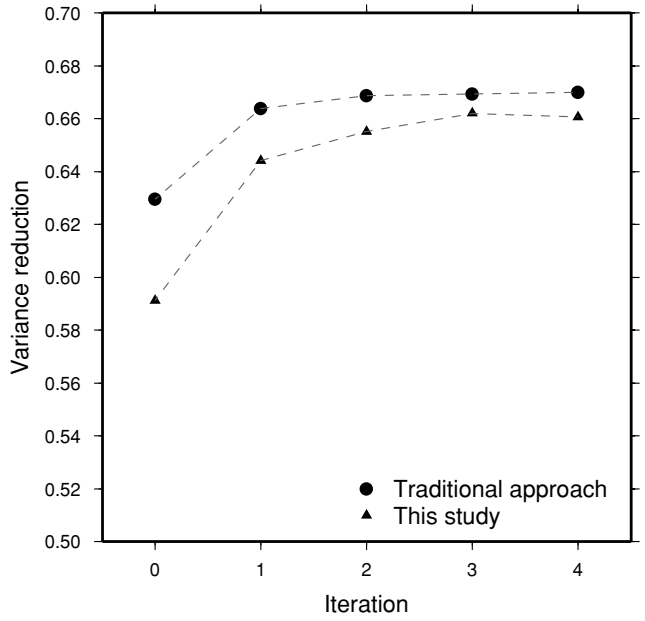

Figure 10. Variance reduction as a function of number of iterations achieved following the traditional approach with 1-D PREM sensitivity kernels (circle) and the improved procedure of this study which makes use of 1-D local sensitivity kernels (triangle).

model and therefore conclude that accurate corrections for shallow-layer features are important to improve our knowledge of parts of the upper mantle where our data have the least sensitivity. For instance, our 3-D anisotropic model derived with this improved approach shows a high velocity anomaly at 300–350 km depth beneath the Western US, possibly the signature of the subducted Juan de Fuca and Farallon slabs, which is barely retrieved, if a standard crustal correction approach is used.

ACKNOWLEDGMENTS

We thank Mark Panning for extensive discussions during the implementation phase of this study. This research was partially supported through a grant from the Stefano Franscini Foundation (Switzerland) and NSF-EAR (Earthscope) grant #0345481. The digital seismograms used in our work have been distributed by the IRIS-DMC, the Geological Survey of Canada and the Northern California Earthquake Data Center (data contributed by the Berkeley Seismological Laboratory, University of California, Berkeley). Contribution number 06-01 of the Berkeley Seismological Laboratory, University of California.

REFERENCES

Bassin, C., Laske, G. & Masters, G., 2000. The current limits of resolution for surface wave tomography in North America, in *EOS, Trans. Am. geophys. Un.*, Vol. 81, p. F897, Fall Meet. Suppl.

Boschi, L. & Ekström, G., 2002. New images of the Earth's upper mantle from measurements of surface wave phase velocity anomalies, *J. geophys. Res.,* **107,** 10.1029/2000JB000059.

Bostock, M. & VanDecar, J., 1995. Upper mantle structure of the Northern Cascadia subduction zone, *Can. J. Earth Sci.,* **32,** 1–12.

Dickinson, W. & Snyder, W., 1979. Geometry of subducted slabs related to San Andreas transform, *J. Geol.,* **87,** 609–627.

Dziewonski, A. & Anderson, D., 1981. Preliminary reference earth model, *Phys. Earth planet. Inter.,* **25,** 297–356.

Ekström, G. & Dziewonski, A., 1998. The unique anisotropy of the Pacific upper mantle, *Nature,* **394,** 168–172.

Humphreys, E. & Dueker, K., 1994. Western U.S. upper mantle structure, *J. geophys. Res.,* **99,** 9615–9634.

Komatitsch, D. & Tromp, J., 1999. Introduction to the spectral element method for three-dimensional seismic wave propagation, *Geophys. J. Int.,* **139,** 806–822.

Li, X. & Romanowicz, B., 1995. Comparison of global waveform inversions with and without considering cross branch coupling, *Geophys. J. Int.,* **121,** 695–709.

Lognonné, P., 1991. Normal modes and seismograms of an anelastic rotating Earth, *J. geophys. Res.,* **96,** 20309–20319.

Lognonné, P. & Romanowicz, B., 1990. Modelling of coupled normal modes of the Earth: the spectral method, *Geophys. J. Int.,* **102,** 365–395.

Marone, F., Gung, Y. & Romanowicz, B., 2006. 3-D radial anisotropic structure of the North American upper mantle from inversion of surface waveform data, *Geophys. J. Int.,* in revision.

Montagner, J.-P. & Jobert, N., 1988. Vectorial tomography; II. Application to the Indian Ocean, *Geophys. J.,* **94,** 309–344.

National Geophysical Data Center, 1988. ETOPO-5, bathymetry/topography data, Data Announc. 88-MGG-02, Natl. Oceanic and Atmos. Admin., U.S. Dep. of Commer., Washington, DC.

Nolet, G., 1990. Partitioned waveform inversion and 2-dimensional structure under the network of autonomously recording seismographs, *J. geophys. Res.,* **95,** 8499–8512.

Panning, M. & Romanowicz, B., 2006. A three dimensional radially anisotropic model of shear velocity in the whole mantle, *Geophys. J. Int.,* **167,** 361–379.

Ritsema, J., Van Heijst, H. & Woodhouse, J., 1999. Complex shear wave velocity structure imaged beneath Africa and Iceland, *Science,* **286,** 1925–1928.

Van der Lee, S. & Nolet, G., 1997. Upper mantle *S*-velocity structure of North America, *J. geophys. Res.,* **102,** 22 815–22 838.

Woodhouse, J. & Dziewonski, A., 1984. Mapping the upper mantle: three dimensional modelling of earth structure by inversion of seismic waveforms, *J. geophys. Res.,* **89,** 5953–5986.

Zhou, Y., Dahlen, F., Nolet, G. & Laske, G., 2005. Finite-frequency effects in global surface-wave tomography, *Geophys. J. Int.,* **163,** 1087–1111.